A Theoretical Mass Transfer Approach for Prediction of Droplets Growth Inside Supersonic Laval Nozzle

Seyed Heydar Rajaee Shooshtari and Akbar Shahsavand[*]
Department of Chemical Engineering, Faculty of Engineering, Ferdowsi University of Mashhad, Mashhad, Iran

Abstract

Proper estimation of droplet growth rate plays a crucial role on appropriate prediction of supersonic separators performance for separation of fine droplets from a gas stream. Up to now, all available researches employ empirical or semi-empirical correlations to define the relationship between droplet growth rate (dr/dt) and other operating variables such as temperatures (T and T_L), Pressure (P) and condensation rate (m_L). These empirical or semi-empirical equations are developed for pure component systems and should not be extended to binary or multi-components systems. A novel theoretical approach is presented in this article which provides a fundamental equation to find the droplet growth rate by resorting to mass transfer equations. The new model uses a combination of mass transfer equations and mass and energy balances to estimate the droplet growth rate, droplet temperature and condensation rate simultaneously. Although the simulation results indicate that the proposed method provides impressive results when validated with several real experimental data, however, the main advantage of the present approach is that it can be easily extended to binary or multi-components systems. To the best of our knowledge, the proposed approach has not been addressed previously.
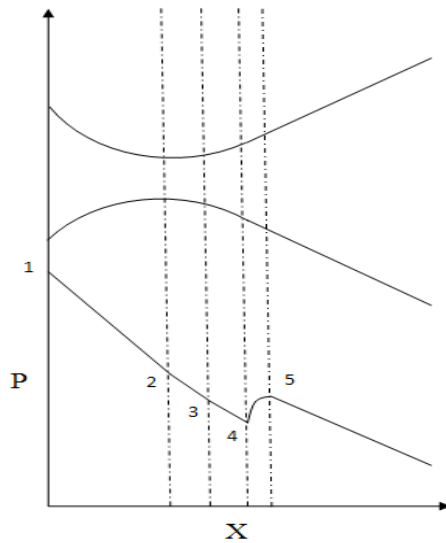
Introduction

Condensation phenomenon in supersonic Laval nozzles is of great importance in many fields such as formation of aerosols, wet steam flows in steam turbines, the flight of aircraft in humid conditions, droplet-spray combustion processes or in phase separation devices (e.g. supersonic separators) [1].

Expansion of a dry gas (such as steam) from superheated to wet condition is composed of several steps. The dry superheated gas initially enters the nozzle (point 1 in Figure 1) and then it expands to the sonic (throat) condition (point 2) during its travel through the nozzle. Evidently, gas pressure and its temperature are drastically reduced due to increase in the gas velocity. Assuming sufficient degree of superheat, the droplet embryos begin to form and grow after the throat (point 3). The pressure drop continues more intensely due to nucleation rate associated with these early embryos and the corresponding droplet growth of previously formed droplets. This area is known as nucleating zone and is terminated by the Wilson point (point 4). Downstream of Wilson point, nucleation ceases effectively and the number of droplets in the flow remains constant. In this region, the droplets grow rapidly and restore the system to the thermodynamic equilibrium. A sudden jump in pressure occurs due to the release of latent heat at supersonic conditions which tends to retard the supersonic flow. Further expansion of the flow takes place close to equilibrium conditions after point 5.

Gyarmathy [2] presented an early model to predict the growth rate over a wide range of pressure and flow regimes from free molecule to continuum. A few years later, Young [1] modified this model by introducing droplet growth parameters α, which presented a relationship between evaporation and condensation coefficients. The corrected model provided better agreement with experiment data in low pressure range and under non-equilibrium condition. He postulated that under non-equilibrium condition, the evaporation coefficient falls below the condensation coefficient during condensation process.

* Corresponding author: Tel. : +98 -915 514 9544,   Fax : +98 -511 8816840   Email: shahsavand@um.ac.ir

Figure 1: Axial pressure distribution in nozzle with spontaneous condensation

Bakhtar and Zidi at 1985 [2] presented a semi-empirical relation for droplet's growth. Gyarmathy [1] presented a fairly realistic approximation for prediction of submicron droplets temperature by considering the capillarity effect and assuming uniform temperature inside the droplets.

Koo et al [3] presented a one-dimensional model based on classical nucleation and growth as a diagnostic tool for predicting the impact of different process conditions and nozzle geometries on particle size distributions produced from supersonic quenching of magnesium vapors.

Among many others, Guha and Young [4], Cinar et al [5], White and Hounslow [6], Dykas [7], Gerber and Kermani [8] , Mahpeykar and Teymourtash [2], Yang and Shen [1] and Dykas and Wroblewski [9] used essentially a similar procedure for estimation of various operating conditions and the corresponding mean droplets radius during the flow of supersonic gas inside Laval nozzle. In all of these researches, the effect of mass transfer on convective heat transfer coefficient is neglected and empirical or semi-empirical correlations are used to determine the relationship between droplet temperature and the fluid temperature in each segment.

In the present article, a novel theoretical approach will be presented which computes the rate of droplet changes during the growth process by resorting to classical mass transfer. The effect of mass transfer on convective heat transfer coefficient will be also considered.

2. A review of traditional mathematical modeling

Proper estimation of the paths typically shown in Figure 1 has crucial effect on the appropriate prediction of supersonic separators performance. Traditional process modeling approach for predicting all profiles of various operating conditions (T_L, T, P, U_G, Ma, J and ρ_G) and the mean droplets radius (r) during the flow of supersonic gas inside Laval nozzle is comprised of the following three sections:

✓ Employment of 5 fundamental equations including mass, momentum and energy balances for the segment under consideration accompanied with Mach number definition and appropriate equation of state for the fluid.
✓ Estimation of number of droplets formed per unit volume per time (J) by resorting to classical nucleation theory (6th equation).
✓ Recruitment of continuity equation and a proper empirical correlation to evaluate the changes of droplets radius and the droplet temperature with time (7th and 8th equation).

Our newly proposed approach uses some steps of the above algorithm while replaces the empirical correlations with an analytical formula derived for prediction of mass transfer rate and its role on the growth rate of condensed droplets. Moreover, a corrected heat transfer coefficient is used to determine the effect of mass transfer on heat transfer rate. Evidently, this correction kicks in when the mass transfer is relatively large.

Assuming one dimensional flow over an incremental distance dx and no inter-phase slip, the fundamental equations for steady

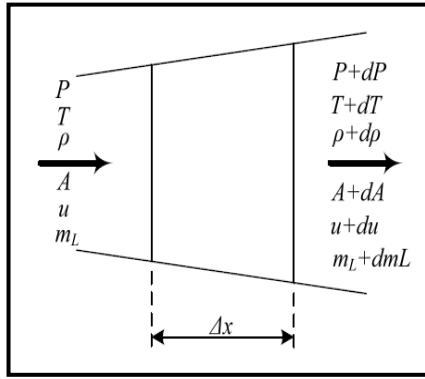state two phase-flow for the segment shown in Figure 2 can be written as [2,5]:

Figure 2: Flow element

2.1. Continuity: Assuming that the area occupied by the liquid droplets is negligible, then continuity equation can be written as:

$$\dot{m}_t = \dot{m}_L + \rho_G A U_G \qquad (1)$$

where $\dot{m}_t$ and $\dot{m}_L$ are the total and liquid mass flow rates respectively, ρ_G is gas density, A is total cross-sectional area of nozzle and U_G is gas velocity. Differentiating equation (1) leads to:

$$\frac{d\rho_G}{\rho_G} + \frac{dA}{A} + \frac{dU_G}{U_G} + \frac{d\dot{m}_L}{\dot{m}_t - \dot{m}_L} = 0 \qquad (2)$$

2.2. Momentum equation: Momentum changes across element dx can be expressed as:

$$d[\dot{m}_G U_G + \dot{m}_L U_L] = -AdP - \frac{f A \rho_G U_G^2}{2d_e} dx \quad (3)$$

Where f is friction factor and d_e is the hydraulic diameter. Assuming no slip occurrence between the phases $(U_G = U_L)$ and dividing equation by $A \times P$, momentum equation can be rearranged as:

$$\frac{dP}{P} = -\frac{f\rho_G U_G^2}{2P} \frac{dx}{d_e} - \frac{m_t U_G}{AP} \frac{dU_G}{U_G} \qquad (4)$$

2.3. Equation of state: Using Virial EOS as:

$$z = \frac{P}{\rho_G \hat{R} T_G} = 1 + B_1 \rho_G + B_2 \rho_G^2 + B_3 \rho_G^3 \qquad (5)$$

where z is compressibility factor, $\hat{R}$ is the universal gas constant on a mass basis

and B_1, B_2, B_3 are viral coefficients which are depended on temperature. After differentiation, equation (5) becomes:

$$\frac{dP}{P} - X \frac{d\rho_G}{\rho_G} - Y \frac{dT_G}{T_G} = 0 \qquad (6)$$

Where

$$X = \frac{\rho_G}{P}\left(\frac{\partial P}{\partial \rho_G}\right)_{T_G}$$

$$= \frac{1 + 2B_1\rho_G + 3B_2\rho_G^2 + 4B_3\rho_G^3}{1 + B_1\rho_G + B_2\rho_G^2 + B_3\rho_G^3}$$

$$Y = \frac{T_G}{P}\left(\frac{\partial P}{\partial T_G}\right)_{\rho_G}$$

$$= 1 + \frac{\rho_G T_G}{1 + B_1\rho_G + B_2\rho_G^2 + B_3\rho_G^3} \times$$

$$\left(\frac{dB_1}{dT_G} + \rho_G \frac{dB_2}{dT_G} + \rho_G^2 \frac{dB_3}{dT_G}\right)$$

2.4. Energy equation: The energy equation for steady state adiabatic flow shown in Figure 2 can be written as:

$$d\left[\dot{m}_G(h_G + \frac{U_G^2}{2}) + \dot{m}_L(h_L + \frac{U_L^2}{2})\right] = 0 \quad (7)$$

Where h_G and h_L are the gas and liquid phase enthalpies, respectively. The change of enthalpy of the vapor phase can be expressed by:

$$dh_G = \left(\frac{\partial h_G}{\partial T_G}\right)_P dT_G + \left(\frac{\partial h_G}{\partial P}\right)_{T_G} dP$$

$$= c_P dT_G + \left[V_G - T_G\left(\frac{\partial V_G}{\partial T_G}\right)_P\right] dP \qquad (8)$$

Dividing equation (7) by $\dot{m}_t c_p T_G$, replacing latent heat $(h_G - h_L)$ with h_{fg}, using equation of state for $\left(\frac{\partial V_G}{\partial T_G}\right)_P$ and equation (1) for $\dot{m}_G$ leads to:

$$\frac{dT_G}{T_G} + \frac{P}{\rho_G c_p T_G}\left(1 - \frac{Y}{X}\right)\frac{dP}{P} + \frac{U_G}{c_p T_G}\frac{dU_G}{U_G}$$

$$- \frac{h_{fg}}{C_p T_G}\frac{d\dot{m}_L}{\dot{m}_t} = 0 \qquad (9)$$

The above equation usually provides the gas temperature at each segment.

2.5. Mach number: The speed of sound in a single phase gas can be expressed as:

$$a = \sqrt{\frac{\gamma P}{\rho_G}} \qquad (10)$$

where γ is the ratio of specific heats. Introducing Z as the square of Mach number value is done as:

$$Z = Ma^2 = \frac{U_G^2 \rho_G}{\gamma P} \qquad (11)$$

Differentiating above equation and rearranging it leads to:

$$\frac{dZ}{Z} = 2\frac{dU_G}{U_G} + \frac{d\rho_G}{\rho_G} - \frac{dP}{P} \qquad (12)$$

2.6. Nucleation rate: Assuming that the initial liquid droplets form only at a critical radius (r^*), then the nucleation rate (J) can be computed by resorting the definition of Dirac-delta function:

$$J(r^*) = \int J^*(r)\delta(r - r^*)\,dr = J^*(r*) \qquad (13)$$

The critical radius (r^*) is given via Kelvin-Helmholtz equation:

$$r^* = \frac{2\sigma}{\rho_L R T_G \ln S} \qquad (14)$$

Where σ is the surface tension and S parameter is the super-saturation ratio. The rate of nucleation is calculated from classical nucleation theory and modified to include non-isothermal effects as: [1]

$$J^* = \frac{q_c}{1 + \eta}\frac{\rho_G^2}{\rho_L}\sqrt{\frac{2\sigma}{\pi m^3}}\exp\left(-\frac{4\pi r^{*2}\sigma}{3kT_G}\right) \qquad (15)$$

Where q_c is the condensation coefficient and has a value between 0.02 and 1.5, *m* is the mass of a single molecule and k is the Boltzmann constant (1.3807×10^{-23} J/K). The non-isothermal correction factor η is defined as:

$$\eta = \frac{2(\gamma - 1)}{1 + \gamma}\frac{h_{fg}}{RT_G}\left(\frac{h_{fg}}{RT_G} - 0.5\right) \qquad (16)$$

2.7. Droplet growth rate and its temperature: Empirical or semi-empirical correlations coupled with energy balance (around a single droplet in the absence of mass transfer) are traditionally used to calculate droplet growth and its temperature inside a Laval nozzle:

Using Young model, the droplet growth rate may be derived on the basis of heat transfer conditions surrounding the droplet as: [1]

$$\frac{dR_d}{dt} = \frac{P}{h_{fg}\rho_L\sqrt{2\pi RT}}\frac{\gamma + 1}{2\gamma}C_p(T_L - T_G) \qquad (17)$$

Where ρ_L and T_L are the liquid density and droplet temperature, respectively. Gyarmathy's provided the following expression for the heat transfer between a stationary droplet and its surrounding for the entire range of Knudsen numbers as: [2]

$$\frac{dR_d}{dt} = \frac{\lambda}{(R_d + 1.59\hat{l})\rho_L}\frac{T_L - T_G}{h_{fg}} \qquad (18)$$

Where λ is the steam thermal conductivity and $\hat{l}$ is the molecular mean free path of steam. Bakhtar and Zidi [2] proposed this semi-empirical relation for prediction of droplet growth rate:

$$\frac{dR_d}{dt} = \left(\frac{K_n}{K_n + 0.375q_c Sc}\right)\frac{q_c}{\rho_L}\left(\frac{R}{2\pi}\right)^{\frac{1}{2}} \times$$
$$\left(\rho_G T_G^{\frac{1}{2}} - \rho_s(T_L, r)T_L^{\frac{1}{2}}\right) \qquad (19)$$

Where K_n is the Knudsen number, *Sc* is the Schmidt number and $\rho_s(T_L, P^{sat}(T_L))$ is saturation density.

Gyarmathy [1] also proposed the following correlation to approximately predict the droplet temperature at each segment.

$$T_L = T^{sat}(P) - \left[T^{sat}(P) - T_G\right]\frac{r^*}{R_d} \qquad (20)$$

Where R_d is mean droplets radius.

Proper combinations of two equations from the above correlations (17-20) can be used to predict the droplet growth rate and its temperature. Some models based on these combinations are shown in Table (1). Equations 2, 4, 6, 9, 12, 15 and various combinations of Table (1) are solved together to calculate the values of unknown parameters T_L, T, P, U_G, Ma, J and ρ_G and

the corresponding mean droplets radius (R_d) at each segment. Fourth order Runge-Kutta method is used in this work in an iterative manner to predict all required profiles. The simulation results for a real case study are presented in the next section.

Table 1: Various combinations for estimation of droplet growth rate and its temperature

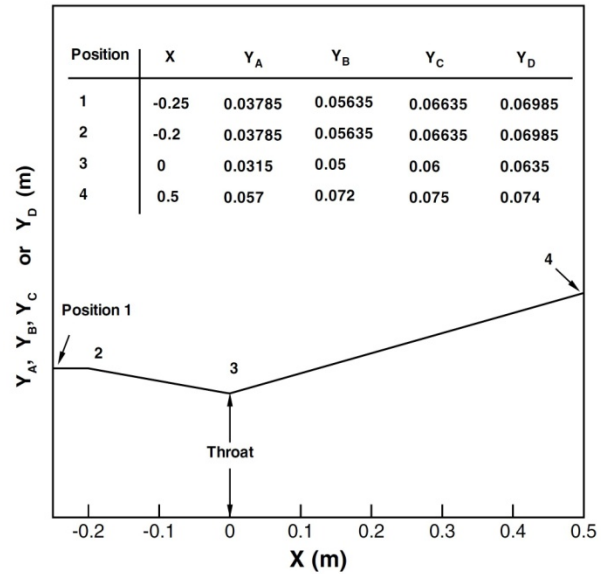| models \ equations	17	18	19	20
1	✓		✓	
2	✓			✓
3		✓	✓	
4		✓		✓
5			✓	✓

3. Real case studies

The experimental data of Moore et al [10,11] and Krol [12,13] are borrowed from literature to investigate the performances of various models presented in Table (1) for computation of droplet growth and its temperature via traditional methods.
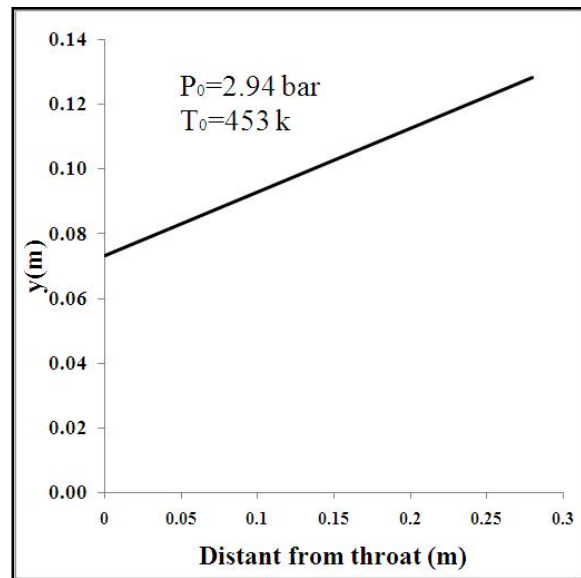
Moor et al nozzle consist of various geometries (A to D) which are shown in Figure 3 and the corresponding stagnation (boundary) conditions for all geometries are presented in Table (2). Detailed geometry and stagnation condition of Krol nozzle is also presented in Figure 4.

Position	X	Y_A	Y_B	Y_C	Y_D
1	-0.25	0.03785	0.05635	0.06635	0.06985
2	-0.2	0.03785	0.05635	0.06635	0.06985
3	0	0.0315	0.05	0.06	0.0635
4	0.5	0.057	0.072	0.075	0.074

Figure 3: Various geometries of converging–diverging nozzles (used by Moor et al [10, 11])

Figure 4: Nozzle geometry and stagnation condition of Krol setup [12, 13])

Table 2: Stagnation (boundary) conditions for various geometries (A to D)

	A	B	C	D
P_0(kpa)	25	25	25	25
T_{G0}(k)	354.6	357.6	358.6	361.8

4. Simulation results for traditional methods

The simulation results of the traditional models (for pressure ratio and mean droplet radius distributions) for the above experimental data are presented in Figures 4 to 7 for various nozzles geometries (A to D) of Moore et al [10,11] and Krol [12,13]. The computed profiles for other parameters especially for the droplet temperature distribution are not included because of the lack of experimental data. As it can be seen, all traditional models of Table 1 perform very similar prediction of pressure ratio distributions along various nozzles of case 1 and 2. But model 5 performs more adequately prediction of mean droplet radius distribution than others (except for nozzle geometry A of Moor et al) for two cases. The next section presents a novel theoretical model based on mass transfer and energy balance equations which can successfully replace all models of Table 1.

5. Theoretical mass transfer approach for prediction of droplet growth rate

Mass balance over a single droplet during growth process inside a Laval nozzle can be written as:

$$\frac{dm_d}{dt} = N_A M_A A \qquad (21)$$

where, m_d is mass of single droplet $\left[m_d = \rho_L \frac{4}{3}\pi r^3 \right]$ and N_A is the molar flux of species A during condensation. For known value of N_A, equation (21) can be used to compute the droplet growth rate. The following section uses a theoretical approach to find the mass transfer flux due to condensation over a spherical droplet.

As shown in Figure (9), mole balance for species A (steam) on a spherical shell of thickness Δr outside of a single droplet can be written as:

$$\frac{d}{dt}\left(4\pi r^2 \Delta r C_A\right) = \left(N_A 4\pi r^2\right)\big|_{r+\Delta r} - \left(N_A 4\pi r^2\right)\big|_r \qquad (22)$$

By resorting to the definition of simple differentiation, rearrangement of equation (22) leads to:

$$r^2 \frac{dC_A}{dt} = \frac{\partial}{\partial r}\left(r^2 N_A\right) \qquad (23)$$

Total mass flux of species A is comprised of two different parts: a) bulk flow and b) mutual diffusion of steam into itself:

$$N_A = N_{Ab} + J_A = N_{Ab} - D_{AA}\frac{dC_A}{dr} \qquad (24)$$

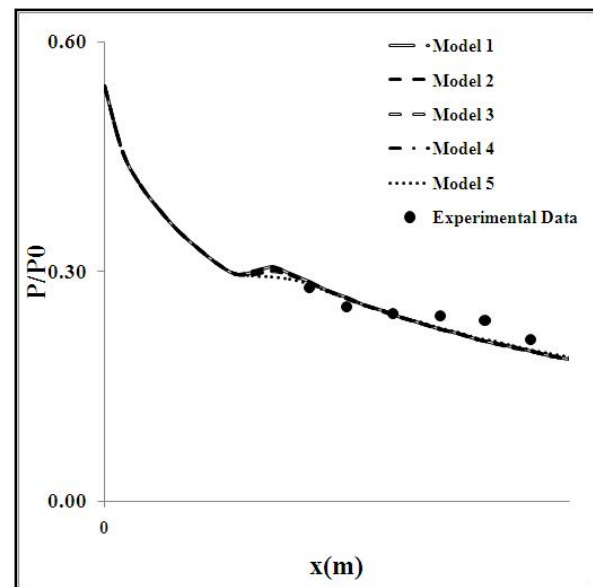where D_{AA} is the self-diffusion coefficient.

Figure 5: Simulation results of traditional methods for prediction of pressure ratio distributions along nozzle of Krol setup
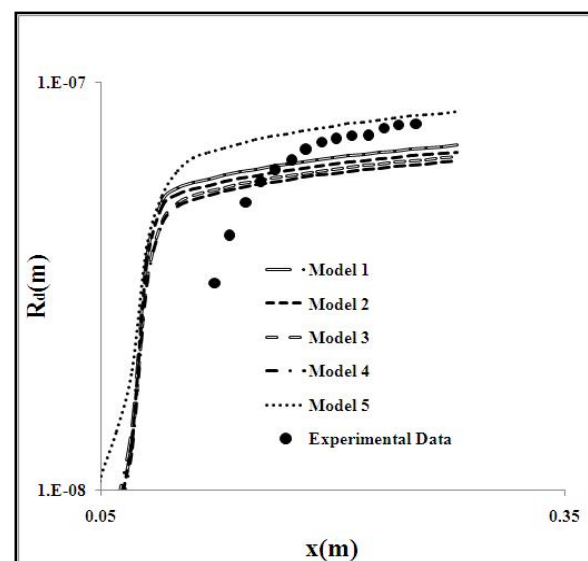

Figure 6: Simulation results of traditional methods for prediction of mean droplet radius distribution along nozzle of Krol setup
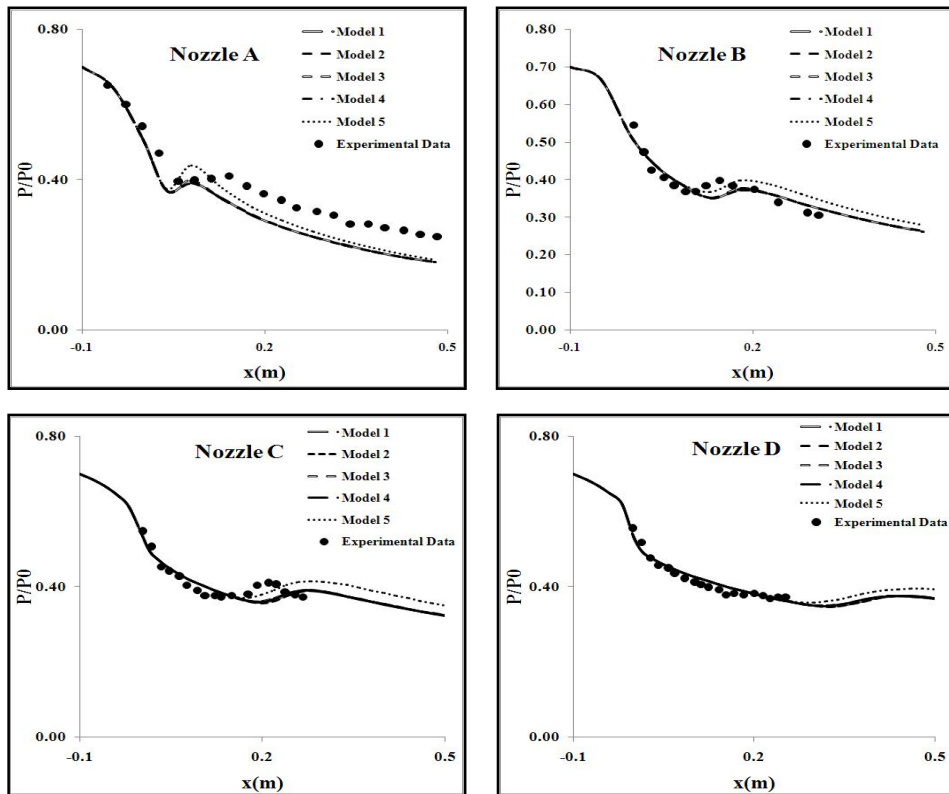
Figure 7: Simulation results of traditional methods for prediction of pressure ratio distributions along various nozzles of Moor et al (A to D)
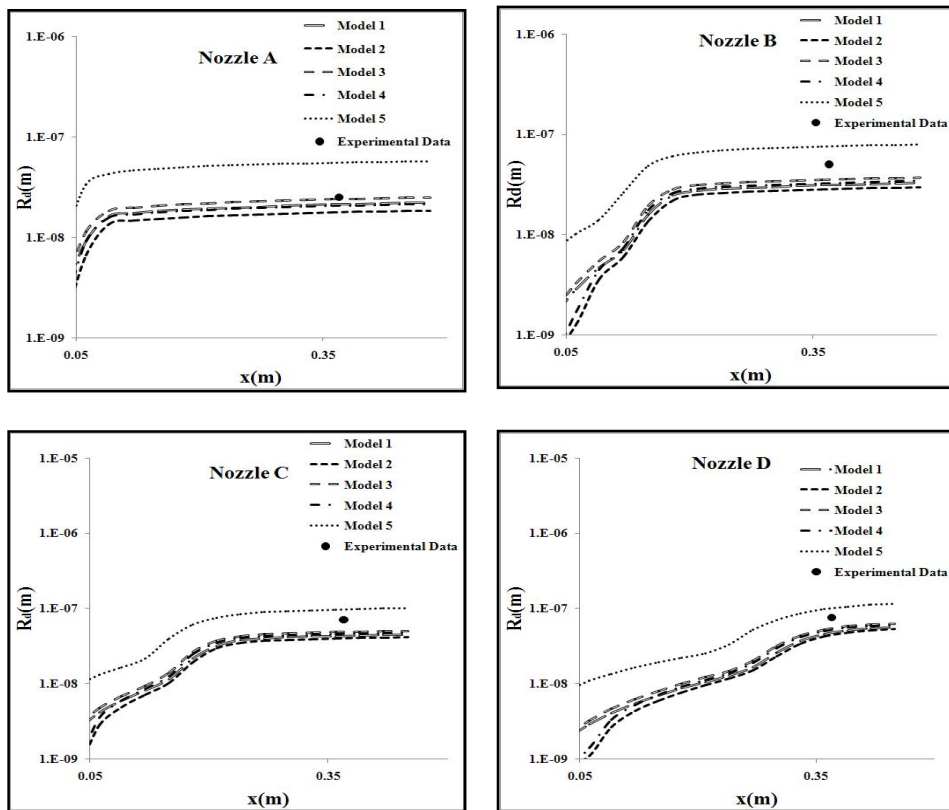

Figure 8: Simulation results of traditional methods for prediction of mean droplet radius distribution along various nozzles of Moor et al (A to D)
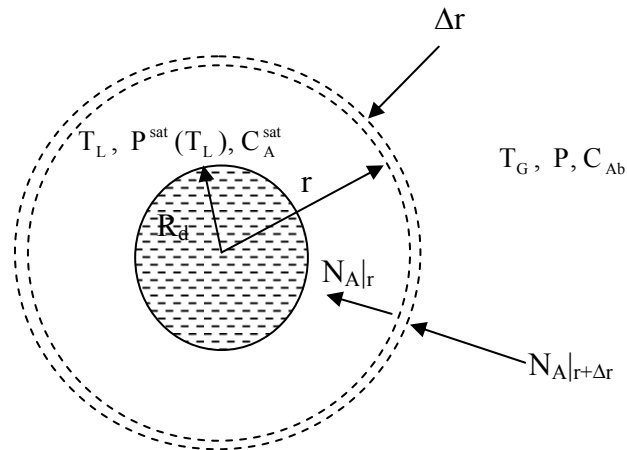
Figure 9: Shell balance for condensation over a single liquid droplet of radius R_d
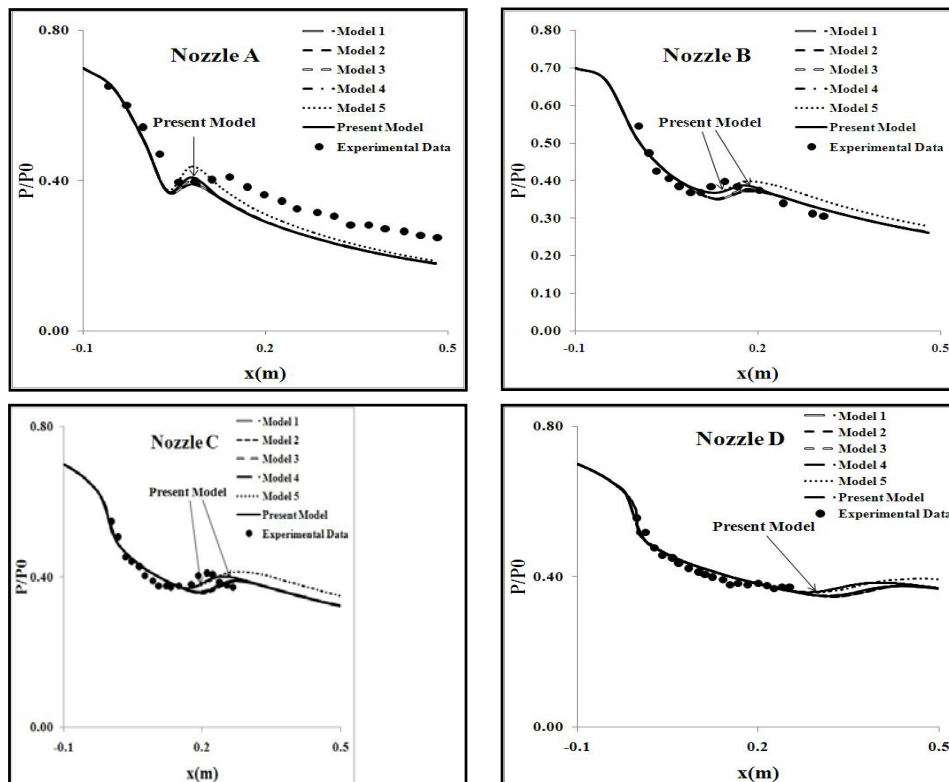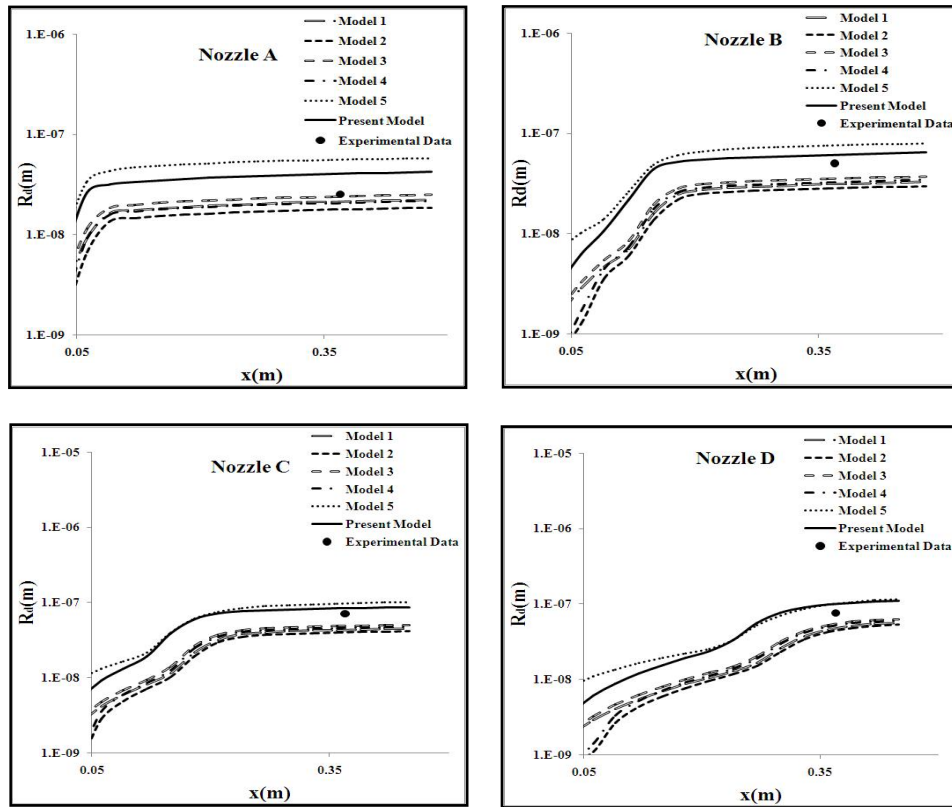

Figure 10: Comparison of present model and traditional methods for prediction of pressure ratio distributions along various nozzles of Moor et al (A to D)

Figure 11: Comparison of present model and traditional methods for prediction of mean droplet radius distribution along various nozzles of Moor et al (A to D)

The convective term in equation (24) (i.e. N_{Ab}) can be neglected due to no inter-phase slip assumption. Substituting for N_A from equation (24) into right hand side term of equation (23) leads to:

$$r^2 \frac{\partial C_A}{\partial t} = -D_{AA}\left(r^2 \frac{\partial^2 C_A}{\partial r^2} + 2r \frac{\partial C_A}{\partial r}\right) \qquad (25)$$

Since r never becomes zero during the growth process, then the above equation reduces to:

$$\frac{\partial C_A}{\partial t} = -D_{AA}\left(\frac{\partial^2 C_A}{\partial r^2} + \frac{2}{r} \frac{\partial C_A}{\partial r}\right) \qquad (26)$$

The above partial differential equation should be solved with the following initial and boundary conditions:

I.C: at t=0 and any r $\quad C_A = C_{Ab}$

B.C.1: at r=R_d and any t $\quad C_A = C_A^{sat}$

B.C.2: at $r \to \infty$ and any t $\quad C_A = C_{Ab}$

Where C_A^* and C_{Ab} are molar concentrations of species A (steam) at the

surface of droplet and bulk of gas stream defined via following equations:

$$C_A^{sat} = \frac{P^{sat}(T_L)}{z(T_L, P^{sat})RT_L} \qquad (27)$$

$$C_{Ab} = \frac{P}{z(T_G, P)RT_G} \qquad (28)$$

Using dimensionless variable $\theta = \frac{C_A - C_{Ab}}{C_A^{sat} - C_{Ab}}$, equation (26) and its initial and boundary conditions become:

$$\frac{\partial \theta}{\partial t} = -D_{AA}\left(\frac{\partial^2 \theta}{\partial r^2} + \frac{2}{r} \frac{\partial \theta}{\partial r}\right) \qquad (29)$$

I.C: at t=0 $\qquad \theta = 0$

B.C.1: at r=R_d $\qquad \theta = 1$

B.C.2: at $r \to \infty$ $\qquad \theta = 0$

Introducing $\psi(r,t) = r.\theta(r,t)$ and using Laplace transform leads to following solution:

$$\frac{C_A - C_{Ab}}{C_A^{sat} - C_{Ab}} = -\frac{R_d}{r} erfc\left(\frac{(r - R_d)}{2\sqrt{D_{AA}t}}\right) \qquad (30)$$

Substituting C_A in equation (24), the condensation (mass transfer) rate over a spherical droplet can be obtained as:

$$N_A = -D_{AA} \frac{dC_A}{dr}\Big|_{r=R_d}$$
$$= D_{AA}\left(C_{Ab} - C_A^{sat}\right)\frac{\sqrt{\pi D_{AA}t} + R_d}{R_d\sqrt{\pi D_{AA}t}} \tag{31}$$

Replacing N_A from above equation into equation (21) results:

$$\frac{dR_d}{dt} = \frac{D_{AA}\dfrac{\sqrt{\pi D_{AA}t} + R_d}{R_d\sqrt{\pi D_{AA}t}}}{\rho_L} \times \tag{32}$$
$$\left(\frac{P}{z\left(T_G, P\right)RT_G} - \frac{P^{sat}\left(T_L\right)}{z\left(T_L, P^{sat}\right)RT_L}\right)$$

The energy balance around a single droplet during its travel inside a Laval nozzle undergoing a condensation process can be formulated as:

$$\frac{d\left(\rho_L \dfrac{4}{3}\pi R_d^3 C_p T_L\right)}{dt} = N_A\left(4\pi R_d^2\right)h_{fg} \tag{33}$$
$$+ \hat{h}\left(4\pi R_d^2\right)\left(T_L - T_G\right)$$

where, $\hat{h}$ is heat transfer coefficient corrected for mass transfer and can be obtained by the following equation: [14]

$$\hat{h} = \frac{\sum N_i C_{Pi}}{1 - e^{-\sum N_i C_{Pi}/h}} \tag{34}$$

The ordinary heat transfer coefficient (h) can be calculated from the empirical correlation presented by Gyarmathy: [2]

$$h = \frac{\lambda}{R_d(1 + 3.18K_n)} \tag{35}$$

where λ is thermal conductivity of steam. Since R_d never becomes zero during the growth process, then equation (33) expands to:

$$\frac{dT_L}{dt} = \frac{3}{R_d}(-T_L \frac{D_{AA}\dfrac{\sqrt{\pi D_{AA}t} + R_d}{R_d\sqrt{\pi D_{AA}t}}}{\rho_L} \times$$
$$\left(\frac{P}{z\left(T_G, P\right)RT_G} - \frac{P^{sat}\left(T_L\right)}{z\left(T_L, P^{sat}\right)RT_L}\right) + \tag{36}$$
$$\frac{D_{AA}\left(\dfrac{P}{z\left(T_G, P\right)RT_G} - \dfrac{P^{sat}\left(T_L\right)}{z\left(T_L, P^{sat}\right)RT_L}\right)h_{fg}}{\rho_L C_p} \times$$
$$\left(\frac{\sqrt{\pi D_{AA}t} + R_d}{R_d\sqrt{\pi D_{AA}t}}\right) + \frac{\hat{h}\left(T_L - T_G\right)}{\rho_L C_p})$$

Equations (32) and (36) replace all combinations of equations (17) to (20) in traditional methods as partially shown in Table 1.

6. Validation of the proposed theoretical model

As before, experimental data of Moore et al [10, 11] and Krol [12, 13] are used to validate the results of the present growth model and compare its performance with the traditional methods. The simulation results obtained by simultaneous solution of equations 2, 4, 6, 9, 12, 15, 32 and 36 are shown in Figures (10) to (13). For comparison purposes, the results of traditional models of Table (1) are also included in these figures. Evidently, the proposed method performs more adequately than traditional models in most cases for prediction of pressure ratio distributions and mean droplet radius profiles along various nozzles geometries.
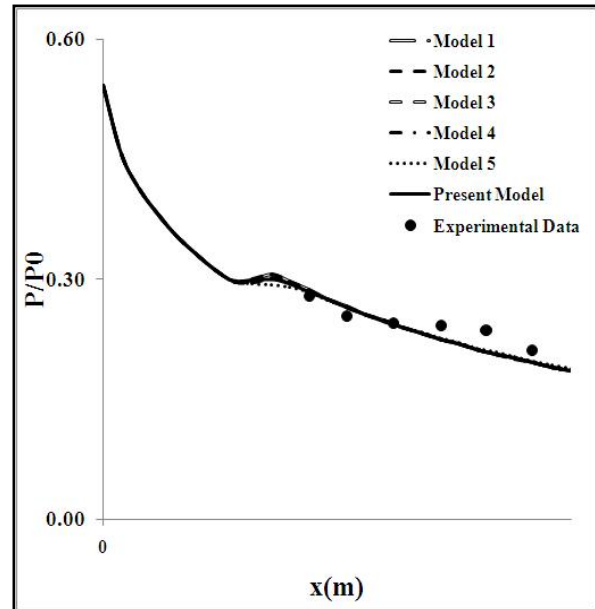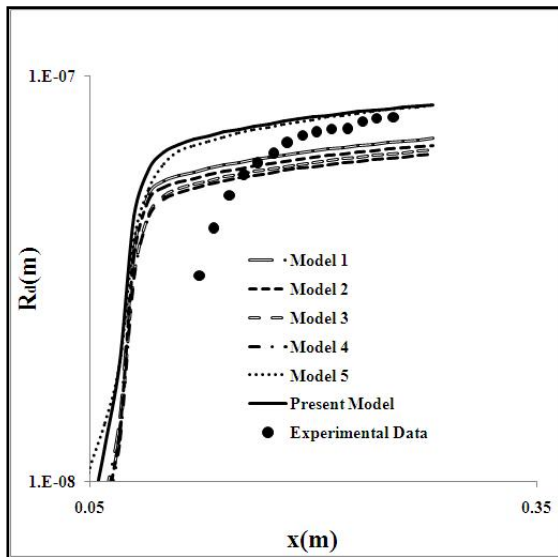
Figure 12: Comparison of present model and traditional methods for prediction of pressure ratio distributions along nozzle of Krol setup

Figure 13: Comparison of present model and traditional methods for prediction of mean droplet radius distribution along nozzle of Krol setup

Conclusion

Numerous empirical correlations are presented in the literature for prediction of liquid droplet growth rate and the corresponding temperature during condensation of a pure component (steam) inside a Laval nozzle. Various combinations of these correlations can be used to simulate the nucleation and growth processes inside a supersonic nozzle. Different combinations of empirical correlations show almost the same performances on prediction of pressure ratio distributions along various nozzles. On the other hand, some combinations perform more adequately estimation of mean droplet radius profile along the Laval nozzles.

None of these conventional empirical or semi-empirical correlations can be extended to binary or multi-components systems. A novel theoretical approach is presented in this article which replaces all combinations of empirical correlations for predictions of pressure ratio and mean droplet radius distributions along with droplet temperature. The proposed method not only very adequately performs for the real case studies borrowed from literature but also, it can be easily extended to binary or multi-components systems.

Nomenclature

A	Area
a	Speed of sound
B	Virial coefficient
C	Concentration
C_p	Specific heat at constant Pressure
D	Diffusion coefficient
D_e	Equivalent diameter
F	Friction factor
h	Enthalpy
h	Heat transfer coefficient
$\hat{h}$	Corrected heat transfer coefficient
h_{fg}	Latent heat
J	Rate of formation of droplets per unit volume and time
J_A	Diffusion rate of species A
k	Boltzmann constant (1.3807×10^{-23} J/K)
K_n	Knudsen number
$\hat{l}$	Mean free path
m	Mass of single molecule
m_d	Mass of single droplet
$\dot{m}_L$	Liquid mass flow rate
$\dot{m}_t$	Total mass flow rate
M_w	Molecular weight
N	Avogadro's number (6.02×10^{23} molecules/mole)
N_A	Mass transfer rate of species A
P	Vapor pressure
$P^{sat}(T_L)$	Saturation pressure at T_L
Q_c	Condensation coefficient
r	Radius
R	Gas constant
$\hat{R}$	Gas constant on a mass basis
R_d	Mean droplet radius
S	Super-saturation ratio
T	Temperature
T_L	Droplet temperature
U	Velocity
γ	Specific heat capacity ratio
μ_G	Kinematic viscosity of vapor
ρ	Density
λ	Coefficient of thermal conductivity
σ	Surface tension
η	non-isothermal correction factor

Subscripts

A	Species A (steam)
b	bulk

G	Vapor phase
L	Liquid phase
in	inlet

Superscripts

| * | Critical droplet |
| sat | saturation |

References:

1- Yang, Y. and Shen, Sh. (2009). "Numerical simulation on non-equilibrium spontaneous condensation in supersonic steam flow." *Int. Commun. Heat. Mass. Tran.*, Vol.36, No. 3, pp. 902–907.

2- Mahpeykar, M.R. and Teymourtash, A.R. (2004). "Effects of friction factor and inlet stagnation conditions on the self-condensation of steam in a supersonic nozzle." *Sci. Iranica*, Vol. 11, No. 4, pp. 269-282.

3- Koo, A. Brooks, G.A. and Nagle, M. (2008). "Nucleation and growth of Mg condensate during supersonic gas quenching." *J. Cryst. Growth*, Vol. 310, No.10, pp. 2659–2667.

4- Guha, A. and Young, J.B. (1991). "Time-marching prediction of unsteady condensation phenomena due to supercritical heat addition." *Proc. conf. on Turbomachinery: Latest Developments in a Changing Scene*, London, pp. 167-177.

5- Cinar,G., Yilbas, B. and Sunar, S. M. (1997). "Study into nucleation of steam during expansion through a nozzle." *Int. J.Multiphas. Flow*., Vol. 23, No. 6, pp. 1171-118.

6- White, A.J. and Hounslow, M.J. (2000). "Modelling droplet size distributions in poly-dispersed wet-steam flows." *Int. J. Heat. Mass. Tran.*, Vol.43, No. 11, pp. 1873-1884.

7- Dykas, S. (2001). "Numerical calculation of the steam condensing flow." *Task quarterly*, Vol.5, No.4, pp. 519–535.

8- Gerber, A.G. and Kermani, M.J. (2004). "A pressure based Eulerian-Eulerian multi-phase model for non-equilibrium condensation in transonic steam flow." *Int. J. Heat. Mass. Tran.*, Vol.47, No.10, pp. 2217–2231.

9- Dykas, S. and Wroblewski, W. (2012). "Numerical modelling of steam condensing flow in low and high-pressure nozzles." *Int. J. Heat. Mass. Tran.*, Vol. 55, No. 21, pp. 6191–6199.

10- Moore, M.J., Walters, P.T., Crane, R.I. and Davidson, B.J. (1973). "Predicting the fog drop size in wet steam turbines", 4th Wet Steam Conf. Institute of Mechanical Engineers (UK), University of Warwick, pp. C37/73.

11- Kermani, M.J. and Gerber, A.G. (2003). "A general formula for the evaluation of thermodynamic and aerodynamic losses in nucleating steam flow." *Int. J. Heat. Mass. Tran.*, Vol.46, No. 17, pp. 3265–3278

12- Krol, T. (1971). "Results of optical measurements of diameters of drops formed due to condensation of steam in a de Laval nozzle(in polish)." *Prace lnstytutu Maszyn Przeplywowych (Trans. Inst. Fluid Flow Machinery)*, Vol.187, pp. 199

13- Bakhtar, F. and Mohammadi Tochai, M. T. (1980). "An Investigation of Two-Dimensional Flows of Nucleating and Wet Steam by the Time-Marching Method." *Int. J. Heat. Fluid Flow*, Vol.2, No. 1, pp. 5–18

14- Treybal, R.E. (1980). "*Mass-Transfer Operations*" 5th.Ed. McGraw-Hill Pub, New York.